Structural Analysis of an Antigen Chemically-Coupled on Virus-Like Particles in Vaccine Formulation

Kristaps Jaudzems, Anna Kirsteina, Tobias Schubeis, Gilles Casano, Olivier Ouari, Janis A Bogans, Andris Kazaks, Kaspars Tars, Anne Lesage, Guido Pintacuda

Structural Analysis of an Antigen Chemically-Coupled on Virus-Like Particles in Vaccine Formulation

Kristaps Jaudzems,*[a] Anna Kirsteina,[b] Tobias Schubeis,[c] Gilles Casano,[d] Olivier Ouari,[d] Janis Bogans,[b] Andris Kazaks,[b] Kaspars Tars,[b] Anne Lesage,*[c] Guido Pintacuda*[c]

[a] Prof. K. Jaudzems
Latvian Institute of Organic Synthesis
Aizkraukles 21, Riga LV-1006 (Latvia)
E-mail: kristaps.jaudzems@osi.lv

[b] A. Kirsteina, J. Bogans, Dr. A. Kazaks, Prof. K. Tars
Latvian Biomedical Research and Study Centre
Ratsupites 1 k1, Riga LV-1067 (Latvia)

[c] Dr. T. Schubeis, Dr. A. Lesage, Dr. G. Pintacuda
Centre de RMN à Très Hauts Champs de Lyon - UMR 5082 (CNRS, ENS Lyon, UCB Lyon 1)
Université de Lyon
F-69100 Villeurbanne (France)
E-mail: anne.lesage@ens-lyon.fr, guido.pintacuda@ens-lyon.fr

[d] Dr. G. Casano, Dr. O. Ouari
Institut de Chimie Radicalaire
AixMarseille Université
F-13013 Marseille (France)

Supporting information for this article is given via a link at the end of the document.

Abstract: Structure determination of adjuvant-coupled antigens is essential for rational vaccine development but has so far been hampered by the relatively low antigen content in vaccine formulations and by their heterogeneous composition. Here we show that magic-angle spinning (MAS) solid-state NMR can be used to assess the structure of the influenza virus hemagglutinin stalk long alpha helix antigen, both in its free, unformulated form and once chemically coupled to the surface of large virus-like particles (VLPs). The sensitivity boost provided by high-field dynamic nuclear polarization (DNP) and proton-detection at fast MAS rates allows to overcome the penalty associated to the antigen dilution. Comparison of the MAS NMR fingerprints between the free and VLP-coupled forms of the antigen provides structural evidence of the conservation of its native fold upon bio-conjugation. This work demonstrates that high-sensitivity MAS NMR is ripe to play a major role in vaccine design, formulation studies and manufacturing process development.

Virus-like particles (VLPs) are empty, non-infectious shells of viruses, which are extensively used in pharmaceutical industry as potent vaccine adjuvants.[1,2] In these applications, the surface of VLPs is typically decorated with antigens from various infectious agents[3–5] or with haptens,[6] increasing by one or two orders of magnitude the antibody titers, and significantly enhancing T-cell and innate immune response.[7] A relevant immune response can however only be provoked if antigens retain their native 3D structure once immobilized on VLPs. The design of efficient vaccines relies therefore on the possibility to characterize the structure of the intermediate and final products during the genetic fusion or bioconjugation steps which are conventionally used to couple protein antigens to the surface of VLPs. Genetic fusion is technically simpler, but it often leads to insoluble or assembly-deficient products, so chemical ligation to free cysteines or lysines is usually the method of choice.[8,9] This protocol yields however assemblies, that are too heterogeneous to be studied by either x-ray crystallography or cryo-EM, and that are too large in size to be investigated by solution NMR.

In this context, magic-angle spinning (MAS) solid-state NMR spectroscopy appears particularly adapted, as this technique can provide structure information in supramolecular biological assemblies independently from their molecular size and the long-range order in the sample formulation.[10,11] A pioneering study in this direction has indeed demonstrated the possibility to characterize a pilot model of protein antigen adsorbed on aluminum hydroxide.[12] The main challenge for MAS NMR structural analysis of surface-coupled antigens is however greatly reduced NMR signal intensity associated with the small relative mass ratio of the antigen compared to the VLP. This problem adds to the difficulties in obtaining tens-of-milligrams labeled sample amounts needed by conventional MAS NMR approaches and to potential heterogeneity introduced by the chemical coupling. These limitations clearly prevent the widespread use of MAS NMR in vaccine research.

Two recent developments in MAS NMR, namely dynamic nuclear polarization (DNP)[13] and ^{1}H-detection at increased magic-angle spinning (MAS) frequencies[14,15] address the sensitivity problem, reducing the amount of sample and the acquisition times needed for a structural analysis. In the context of vaccine research, proton-detected solid-state NMR spectroscopy under 100 kHz MAS frequency has recently allowed the structural determination of 2.5 MDa VLP with sub-milligrams sample quantities.[16] In parallel, DNP-enhanced MAS NMR has been successfully applied to reveal multiple conformations of lipid-anchored peptides[17] as well as the adsorption mode of antigens onto aluminum-based adjuvants.[18]

Here we take advantage of both approaches to perform the structural analysis of the influenza virus hemagglutinin (HA) stalk long alpha helix (LAH) antigen coupled to the surface of a VLP. We first use conventional MAS NMR to determine the 3D structure of the free antigen in microcrystalline form. We then exploit the sensitivity boost provided by proton detection and high-field DNP to assess the integrity of the antigen structure after the attachment onto the VLP surface, as well as to identify the structurally divergent regions. To our best knowledge, this work

represents the first example of an atomic level structural analysis of a VLP-coupled protein.

The HA stalk LAH is one of the most conservative influenza virus antigens and is being investigated as a potential universal influenza vaccine component.[19] The immunogenic form of the protein is an α-helical trimer resembling the corresponding region of native HA in its post-fusion form.[20] We studied a short, N-terminally truncated version of the LAH antigen comprising HA residues 418-474. A high-resolution (1.34 Å) crystal structure of the LAH trimer was determined as a reference and to assist resonance assignment of MAS NMR spectra (Figure S1).

To increase antibody titers and obtain a stronger T-cell response, the antigen was coupled to VLPs of ssRNA bacteriophage Qβ (Figure 1), which have been used previously in vaccine development.[6,21,22] Uniformly (U)-^{13}C,^{15}N-labeled LAH antigen (HA residues 418-474) was produced by expression in *Escherichia coli* and purified as described in Supporting information. The free form of the protein was precipitated using saturated ammonium sulphate. The coupling of labeled LAH antigen to unlabeled Qβ VLPs was performed via SATA–maleimide conjugation chemistry (Figure S2) and the resulting product was sedimented by ultra-centrifugation.[23,24]

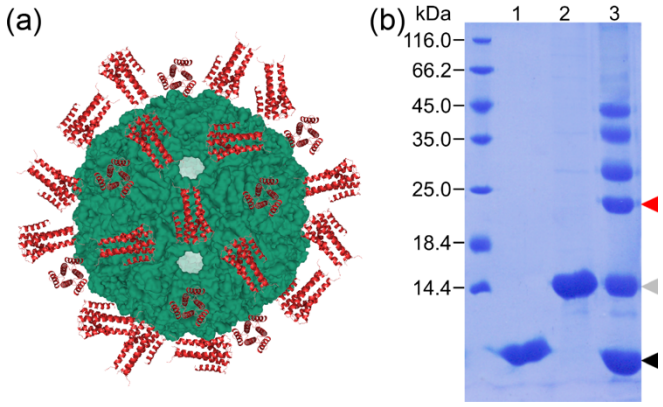

Figure 1. (a) Structural model of LAH antigen coupled to the surface of Qβ VLP. (b) SDS-PAGE analysis of the coupling reaction: lanes 1 and 2 – HA stalk LAH and Qβ coat proteins before coupling; lane 3 – after coupling. Red arrow refers to the coupling zone, grey arrow – coat protein monomer, black arrow – HA stalk LAH protein. Coupling bands indicate a successful reaction.

We started our study with the ^{13}C and ^{15}N chemical shift assignment of free LAH antigen by recording ^{13}C-detected experiments at moderate MAS frequencies (12.5–20 kHz in a 3.2 mm rotor) on a U-^{13}C,^{15}N-labeled sample. An excellent spectral quality was observed in the 2D RFDR[25] and DARR[26] spectra (Figure S3), where isolated resonances displayed line widths of ~0.7 ppm. The backbone and side chain assignment was completed for residues 5–58, except for L30, L46, L54, K55 using 3D NCOCX, NCACX, CONCA and CANCO spectra (Figure S4). Figure 2a-b shows the assigned 2D NCO and NCA spectra.

Further, to obtain the ^{1}H chemical shift assignments we recorded experiments to correlate the ^{15}N and ^{13}C chemical shifts to those of their bound ^{1}H nuclei. To this end, we repacked the sample of free LAH antigen in a 0.7 mm rotor and acquired 3D (H)NCAH, (H)CBCAH, (H)COCAH and (H)CCH spectra[27] with 105 kHz MAS. Analysis of these spectra allowed assignment of the resonances of most Hα nuclei as well as of side chain protons (Figure 2c, Figure S5).

To determine the secondary structure elements, deviations of our assigned ^{13}Cα,β chemical shifts from random-coil values were analyzed (Figure 3a). This procedure predicted two helices with locations almost identical to those in the crystal structure, except that the helix 2 appeared to be shorter near the C-terminus by two residues. Further, to verify the same relative positioning of the two helices, we calculated the expected intra-molecular inter-residual H-H contacts <5 Å from the crystal structure and checked their manifestation in the 2D C(HH)C and N(HH)C spectra (Figure 3b-c). A total of 689 (out of 1334) contacts were confirmed in this way including 297 sequential, 314 medium-range (2-4 residues apart) and 78 long-range (5 and more residues apart) contacts, which indicates a good fit between the MAS NMR data and the crystal structure.

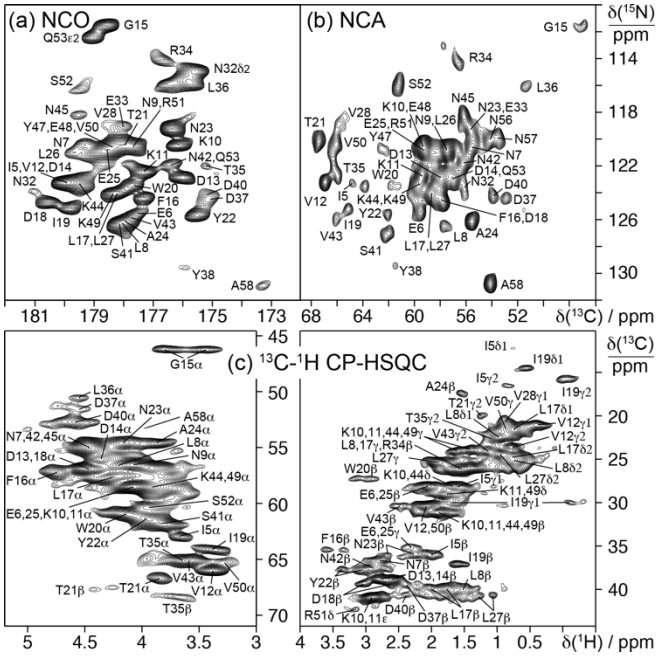

Figure 2. Chemical shift assignment of free LAH antigen. (a) and (b) Assigned NCO and NCA spectra of U-^{13}C,^{15}N-labeled LAH antigen at 800 MHz with 17 kHz MAS. (c) Assigned ^{1}H-detected 2D ^{13}C,^{1}H CP-HSQC spectra of U-^{13}C,^{15}N-labeled free LAH antigen at 1 GHz with 105 kHz MAS.

Finally, we calculated the 3D structure of the LAH trimer subunit using CYANA[28] with the confirmed H-H contacts as upper-limit distance restraints of 5 Å and backbone torsion angle (ψ, φ) restraints derived from chemical shifts using TALOS.[29] Notably, because cross peaks observed from a U-^{13}C,^{15}N-labeled sample can arise from both intra-molecular and inter-molecular contacts the quaternary structure could not be determined based on these data. Although the inter-molecular contacts were ignored, our calculation converged to a single structure. The obtained structure is well defined, except for the first four and the last four residues, and agrees well with the crystal trimer subunit yielding a backbone heavy-atom RMSD of 0.89 Å, when superimposed (Figure 3d).

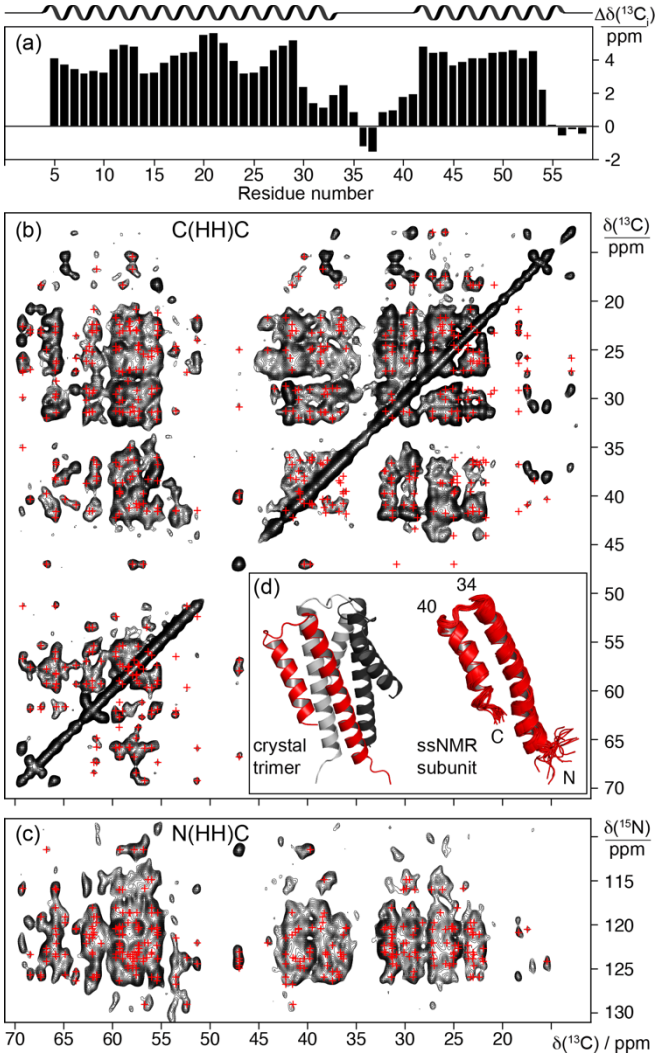

Figure 3. Secondary and tertiary structure of free LAH antigen. (a) ^{13}Cα and ^{13}Cβ chemical shift deviations from random-coil values in LAH antigen. $\Delta\delta(^{13}C_i)$ values above 1 are indicative of helices, while values below -1 indicate β-strand or extended structure. The $\Delta\delta(^{13}C_i)$ value for each residue i was determined as an average over three residues. Locations of helices in the crystal structure of LAH trimer are indicated above the plot. (b) and (c) Expansion of 2D C(HH)C and N(HH)C spectra of U-^{13}C,^{15}N-labeled LAH antigen at 800 MHz with 20 kHz MAS. Confirmed inter-residual H-H proximities <5 Å expected based on the crystal structure of LAH trimer are indicated with a red cross. (d) MAS NMR structure of LAH trimer subunit and comparison with the crystal structure.

Once coupled to VLP, we estimate that the LAH antigen occupies no more than ~10% of the sample volume (see Figure S2). In order to overcome the associated sensitivity drop, and allow a structural comparison of the free and VLP-coupled LAH antigen in reasonable experimental times, DNP-enhanced and proton-detected MAS NMR were employed.

DNP-enhanced NMR was applied at 800 MHz with 40 kHz MAS in a 1.3 mm rotor and under cryogenic temperatures. The sample was doped with the polarizing agent M-TinyPol,[30] which allows to conjugate the advantages of high magnetic fields and fast MAS[31] with large sensitivity enhancements. In these conditions, a sensitivity enhancement of about 40 was notably observed for the resonances of the VLP-coupled dilute LAH antigen (Figure S6), which enables the acquisition of sensitive 2D carbon-carbon fingerprints in 38 hours. Panels a-c of Figure 4 show expansions of the overlaid 2D ^{13}C–^{13}C dipolar correlation spectra of free and VLP-coupled LAH antigen acquired using DNP NMR.

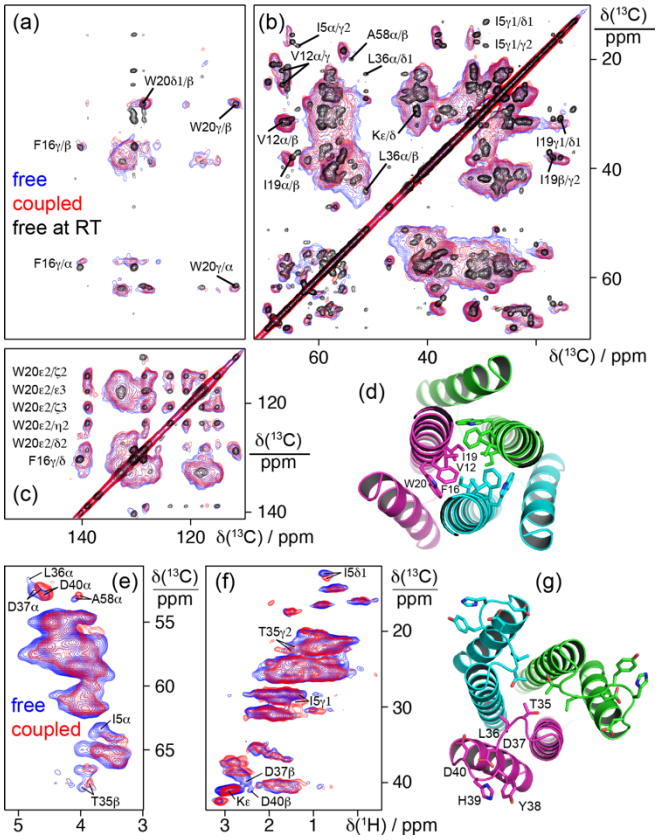

Figure 4. Comparison of free and VLP-coupled LAH antigen. (a), (b) and (c) Overlays of different spectral regions from DNP-enhanced 2D CORD spectra of U-^{13}C,^{15}N-labeled free (blue) and VLP-coupled (red) LAH antigen at 800 MHz and 115 K with 40 kHz MAS with the room temperature 2D DARR spectrum of free LAH antigen (black) at 800 MHz with 20 kHz MAS. (d) Crystal structure of LAH antigen showing the side chains of V12, F16, I19 and W20 that make up the hydrophobic core of the trimer. (e) and (f) Overlays of Hα-Cα and side chain regions from ^{1}H-detected 2D ^{13}C,^{1}H CP-HSQC spectra of U-^{13}C,^{15}N-labeled free (blue) and VLP-coupled (red) LAH antigen at 1 GHz with 60 kHz MAS. (g) Crystal structure of LAH trimer showing the side chains of residues T35-D40 in the loop between helices 1 and 2.

In parallel, 2D ^{1}H-detected CP-HSQC experiments (with a theoretical sensitivity gain by a factor of ~8 with respect to direct ^{13}C acquisition) were recorded at 1 GHz and at ambient temperature, in 1 hour. Experiments were carried out at intermediate spinning speeds (60 kHz) and rotor size (1.3 mm) which represents in our hands the best compromise between absolute sensitivity and resolution. Despite the lower expected sensitivity gain, the ^{1}H-detected experiments allow monitoring the ^{1}H NMR resonances that are more sensitive to small structural and environmental changes given the peripheral location of proton nuclei in proteins. Panels e-f show expansions of the overlaid 2D ^{13}C–^{1}H dipolar correlation spectra of the two forms. DNP-enhanced 2D ^{15}N-^{13}C and ^{1}H-detected 2D ^{15}N-^{1}H dipolar correlations were also recorded but were not sufficiently resolved for site-specific analysis (Figure S7). With respect to the DNP spectra, we note that sample freezing induces a substantial line broadening (cf. the room temperature spectrum of the free form

superimposed in black) and causes the disappearance of several signals corresponding to the most dynamically disordered segments that are frozen out in different conformations under DNP conditions. This is the case for the first assigned N-terminal residue I5 and the C-terminal A58 (visible in INEPT spectrum, see Figure S6c) as well as part of cross-peaks from L36 located in the loop between helix 1 and 2, all of which are expected to exhibit significant mobility at ambient temperature.

The DNP-enhanced and proton-detected NMR fingerprints report on the 3D structural identity at atomic level of LAH trimer before and after chemical coupling to the VLP surface. In particular, the two pairs of spectra are virtually identical both in regions containing isolated peaks and also in the most crowded areas where the intensity distribution is unchanged. Notably, several well-resolved cross-peaks from residues V12, F16, I19 and W20 forming the hydrophobic core of the trimer (Figure 4d) feature a perfect overlap between the two forms in the DNP-enhanced NMR spectra, confirming that the trimeric fold of LAH antigen is preserved in its VLP-coupled form. Although the chemical coupling involved modification of the amino group of lysines, no indication of heterogeneity (e.g. peak doubling of Hε/Cε correlations) could be seen in the spectra. At the same time a small number of signals are either shifted or lose intensity upon the coupling in the proton-detected CP-HSQC spectra. These signals correspond to the dynamical regions of the antigen, which are invisible under DNP at cryogenic temperature, and include peaks from the first assigned N-terminal residue I5 and the C-terminal A58 as well as from residues T35, L36, D37 and D40 located in the loop between helix 1 and 2. This likely reports on variations due to different aggregation states. For example, intermolecular contacts in the microcrystalline preparation are abrogated upon coupling to the VLP, as in the X-ray structure trimers pack with the loops against each other. The possibility to spot such interactions is a particular strength of the method as they may affect the availability of the antigen with an overall impact on the efficiency of the vaccine formulation.

In summary, MAS NMR spectroscopy was used to investigate the structure of the HA stalk LAH antigen both in free form and coupled to the surface of a VLP. Notably, the sensitivity and resolution afforded by high-field DNP-enhanced and ^{1}H-detected MAS NMR were sufficient for an atomic-level structural screening of the antigen with the extreme dilution imposed by the fusion with the large VLP carrier. The results revealed a high structural similarity of the free and coupled forms, with noticeable differences being limited to the less well-structured regions near the N and C termini and in the inter-helix loop confirming the preservation of the trimeric helix bundle of the LAH antigen in the vaccine formulation.

The MAS NMR methodology described in this work is expected to be valuable beyond applications in vaccine development, since the characterization of biomolecules upon chemical coupling is a common problem in many biotechnology problems. Some examples include covalent linking of enzymes to antibodies, protein labeling and exposure of “addresses” on the surface of protein nanocontainers. We expect that MAS NMR with high sensitivity will be able to contribute to the structure determination of the different components after bioconjugation in these many different areas.

Acknowledgements

We acknowledge funding from Egide (Osmosis project n 39719WH), State Education and Development Agency of Latvia (Osmoze project no. LV-FR/2018/2) and ERDF project 1.1.1.1/16/A/054 "Diagnostic and immunoprotective potential of influenza virus hemagglutinin stalk peptide: generation of novel vaccine prototypes". The work was additionally funded by the European Research Council (ERC-2015-CoG GA 648974 to GP), and access to high-field NMR was cofunded by the CNRS (IR-RMN FR3050) and by the EC (project iNext GA 653706). Financial support from Equipex contracts ANR-10-EQPX-47-01 and ANR-15-CE29-0022-01 is gratefully acknowledged.

Keywords: Antigen structure • virus-like particle • vaccine development • solid-state NMR • dynamic nuclear polarization

[1] M. F. Bachmann, G. T. Jennings, *Nat. Rev. Immunol.* **2010**, *10*, 787–796.
[2] M. F. Bachmann, U. H. Rohrer, T. M. Kündig, K. Bürki, H. Hengartner, R. M. Zinkernagel, *Science* **1993**, *262*, 1448–1451.
[3] A. Kirsteina, I. Akopjana, J. Bogans, I. Lieknina, J. Jansons, D. Skrastina, T. Kazaka, K. Tars, I. Isakova-Sivak, D. Mezhenskaya, T. Kotomina, V. Matyushenko, L. Rudenko, A. Kazaks, *Vaccines (Basel)* **2020**, *8*, DOI 10.3390/vaccines8020197.
[4] A. L. Marcinkiewicz, I. Lieknina, S. Kotelovica, X. Yang, P. Kraiczy, U. Pal, Y.-P. Lin, K. Tars, *Front. Immunol.* **2018**, *9*, 181.
[5] M. F. Bachmann, A. Zeltins, G. Kalnins, I. Balke, N. Fischer, A. Rostaher, K. Tars, C. Favrot, *J. Allergy Clin. Immunol.* **2018**, *142*, 279-281.e1.
[6] J. Cornuz, S. Zwahlen, W. F. Jungi, J. Osterwalder, K. Klingler, G. van Melle, Y. Bangala, I. Guessous, P. Müller, J. Willers, P. Maurer, M. F. Bachmann, T. Cerny, *PLoS ONE* **2008**, *3*, e2547.
[7] G. T. Jennings, M. F. Bachmann, *Biol. Chem.* **2008**, *389*, 521–536.
[8] Z. Chen, D. L. Stokes, W. J. Rice, L. R. Jones, *J. Biol. Chem.* **2003**, *278*, 48348–48356.
[9] R. J. Duncan, P. D. Weston, R. Wrigglesworth, *Anal. Biochem.* **1983**, *132*, 68–73.
[10] J.-P. Demers, P. Fricke, C. Shi, V. Chevelkov, A. Lange, *Prog. Nucl. Magn. Reson. Spectrosc.* **2018**, *109*, 51–78.
[11] C. M. Quinn, M. Wang, T. Polenova, *Methods Mol. Biol.* **2018**, *1688*, 1–35.
[12] L. Cerofolini, S. Giuntini, E. Ravera, C. Luchinat, F. Berti, M. Fragai, *NPJ Vaccines* **2019**, *4*, 20.
[13] K. Jaudzems, T. Polenova, G. Pintacuda, H. Oschkinat, A. Lesage, *J. Struct. Biol.* **2019**, *206*, 90–98.
[14] L. B. Andreas, T. Le Marchand, K. Jaudzems, G. Pintacuda, *J. Magn. Reson.* **2015**, *253*, 36–49.
[15] A. Böckmann, M. Ernst, B. H. Meier, *J. Magn. Reson.* **2015**, *253*, 71–79.
[16] L. B. Andreas, K. Jaudzems, J. Stanek, D. Lalli, A. Bertarello, T. Le Marchand, D. Cala-De Paepe, S. Kotelovica, I. Akopjana, B. Knott, S. Wegner, F. Engelke, A. Lesage, L. Emsley, K. Tars, T. Herrmann, G. Pintacuda, *Proc. Natl. Acad. Sci. U.S.A.* **2016**, *113*, 9187–9192.
[17] E. J. Koers, M. P. López-Deber, M. Weingarth, D. Nand, D. T. Hickman, D. Mlaki Ndao, P. Reis, A. Granet, A. Pfeifer, A. Muhs, M. Baldus, *Angew. Chem. Int. Ed. Engl.* **2013**, *52*, 10905–10908; *Angew. Chem.* **2013**, *125*, 11106-11109.
[18] J. Viger-Gravel, F. M. Paruzzo, C. Cazaux, R. Jabbour, A. Leleu, F. Canini, P. Florian, F. Ronzon, D. Gajan, A. Lesage, *Chemistry* **2020**, DOI 10.1002/chem.202001141.
[19] Y. H. Jang, B. L. Seong, *Front. Cell. Infect. Microbiol.* **2019**, *9*, 344.
[20] I.-N. Lu, A. Kirsteina, S. Farinelle, S. Willieme, K. Tars, C. P. Muller, A. Kazaks, *PLoS ONE* **2018**, *13*, e0204776.
[21] A. C. Tissot, P. Maurer, J. Nussberger, R. Sabat, T. Pfister, S. Ignatenko, H.-D. Volk, H. Stocker, P. Müller, G. T. Jennings, F. Wagner, M. F. Bachmann, *Lancet* **2008**, *371*, 821–827.
[22] K.-M. Beeh, F. Kanniess, F. Wagner, C. Schilder, I. Naudts, A. Hammann-Haenni, J. Willers, H. Stocker, P. Mueller, M. F. Bachmann, W. A. Renner, *J. Allergy Clin. Immunol.* **2013**, *131*, 866–874.

[23] I. Bertini, C. Luchinat, G. Parigi, E. Ravera, B. Reif, P. Turano, *Proc. Natl. Acad. Sci. U.S.A.* **2011**, *108*, 10396–10399.

[24] C. Gardiennet, A. K. Schütz, A. Hunkeler, B. Kunert, L. Terradot, A. Böckmann, B. H. Meier, *Angew. Chem. Int. Ed. Engl.* **2012**, *51*, 7855–7858; *Angew. Chem.* **2012**, *124*, 7977-7980.

[25] A. E. Bennett, R. G. Griffin, J. H. Ok, S. Vega, *J. Chem. Phys.* **1992**, *96*, 8624–8627.

[26] K. Takegoshi, S. Nakamura, T. Terao, *Chem. Phys. Lett.* **2001**, *344*, 631–637.

[27] J. Stanek, L. B. Andreas, K. Jaudzems, D. Cala, D. Lalli, A. Bertarello, T. Schubeis, I. Akopjana, S. Kotelovica, K. Tars, A. Pica, S. Leone, D. Picone, Z.-Q. Xu, N. E. Dixon, D. Martinez, M. Berbon, N. El Mammeri, A. Noubhani, S. Saupe, B. Habenstein, A. Loquet, G. Pintacuda, *Angew. Chem. Int. Ed. Engl.* **2016**, *55*, 15504–15509; *Angew. Chem.* **2016**, *128*, 15730-15735.

[28] P. Güntert, C. Mumenthaler, K. Wüthrich, *J. Mol. Biol.* **1997**, *273*, 283–298.

[29] Y. Shen, F. Delaglio, G. Cornilescu, A. Bax, *J. Biomol. NMR* **2009**, *44*, 213–223.

[30] A. Lund, G. Casano, G. Menzildjian, M. Kaushik, G. Stevanato, M. Yulikov, R. Jabbour, D. Wisser, M. Renom-Carrasco, C. Thieuleux, F. Bernada, H. Karoui, D. Siri, M. Rosay, I. V. Sergeyev, D. Gajan, M. Lelli, L. Emsley, O. Ouari, A. Lesage, *Chem. Sci.* **2020**, *11*, 2810–2818.

[31] K. Jaudzems, A. Bertarello, S. R. Chaudhari, A. Pica, D. Cala-De Paepe, E. Barbet-Massin, A. J. Pell, I. Akopjana, S. Kotelovica, D. Gajan, O. Ouari, K. Tars, G. Pintacuda, A. Lesage, *Angew. Chem. Int. Ed. Engl.* **2018**, *57*, 7458–7462; *Angew. Chem.* **2018**, *130*, 7580-7584.

Entry for the Table of Contents

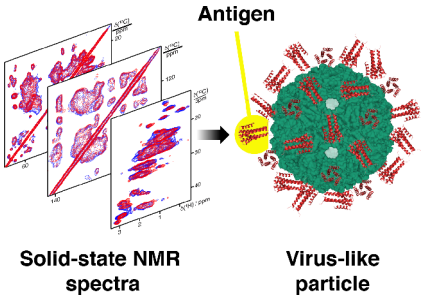

In situ vaccine antigen structural analysis: The sensitivity boost provided by dynamic nuclear polarization and proton detection with fast magic-angle spinning renders solid-state NMR capable of structural analysis in heterogeneous vaccine formulations with dilute adjuvant-coupled antigens. We demonstrate this methodology on the influenza virus hemagglutinin stalk long alpha helix antigen after coupling to virus-like particles.

Institute and/or researcher Twitter usernames: @KrJaudzems (Kristaps Jaudzems), @osi_lv (Latvian Institute of Organic Synthesis)